INTERNATIONAL JOURNAL FOR NUMERICAL METHODS IN FLUIDS, VOL. 8, 1051–1070 (1988)

NON-LINEAR FREE SURFACE FLOWS AND AN APPLICATION OF THE ORLANSKI BOUNDARY CONDITION

SRIDHAR JAGANNATHAN

The Glosten Associates, Inc., Seattle, Washington 98104, U.S.A.

SUMMARY

The focus of this paper is the analysis of spatially two-dimensional non-linear free surface problems. The critical aspects of the problem concern the treatment of the non-linear free surface, the body boundary condition for large motions and the imposition of suitable radiation conditions. To address such complexities, time domain simulation was chosen as the method of analysis. With the use of a finite domain for simulation, a major concern is with the radiation condition to be applied at the open or truncation boundary. For the two-dimensional problem at hand, no theoretical radiation conditions are known to exist. An extension of the Orlanski open boundary condition, based on phase velocity determination at the free surface, is proposed. Three categories of problems were analysed using numerical simulation—namely, freely moving steep waves, waves over a submerged body and forced body motion. Simulation results have been compared with linear theory and experiments.

KEY WORDS Simulation Non-linear Free Surface Open Boundary Condition

1. INTRODUCTION

The particular hydrodynamic problem of interest here is that of a two-dimensional submerged body in close proximity to the free surface subject either to an incident wave or to a forced motion. The domain equation for the velocity potential, assuming the fluid to be inviscid and incompressible and the flow irrotational, is the Laplace equation which is linear. Non-linearities are introduced into the problem through the boundary conditions at the free surface and on the body. Distinct from the frequency domain perturbation approach, much effort in recent years has gone into treating the free surface and body non-linearities directly in the time domain. A comprehensive review of numerical methods in free surface flows is given by Yeung.[1]

A new era in non-linear free surface calculations was initiated by Longuet-Higgins and Cokelet[2] in their simulation of unsteady two-dimensional waves. The waves are considered spatially periodic and the free surface is mapped into a closed contour. A Fredholm integral equation of the first kind is set up for the velocity potential and its normal for marker particles on the free surface. Hence at every instant in time the velocity field for each marker particle is known through spatial differentiation. This permits the Lagrangian dynamic and kinematic free surface conditions to serve as evolution equations for the velocity potential and position for each marker particle. This then sets up the boundary value problem for the next instant in time. This method is remarkably simple and effective and has the added advantage that the marker particles become concentrated near regions of sharp curvature. Vinje and Brevig[3] modified the method of Longuet-

0271–2091/88/091051–20$10.00

Received 17 June 1987
Revised 23 November 1987

Higgins and Cokelet and, by using Cauchy's theorem, formulated the problem in terms of a Fredholm integral equation of the second kind for the velocity potential and the stream function. Subsequently Vinje and Brevig[4, 5] analysed a variety of body–fluid interaction problems using this method.

2. MATHEMATICAL FORMULATION

The problem is posed as an initial value problem concerning the forced motion of a two-dimensional body in proximity to the free surface. Exact boundary conditions are to be imposed on the free surface and on the body. Figure 1 shows a definition sketch for the problem. The fluid domain consists of the free surface, the body, the bottom and two computational or 'open boundaries'. The method of solution to be used is based on a semi-Lagrangian time-stepping procedure first used by Longuet-Higgins and Cokelet.[2] This procedure permits the satisfaction of the non-linear dynamic and kinematic free surface conditions. Vinje and Brevig[3] modified this procedure for solutions in the physical plane. This modified method will be used as the basic technique for the solution of the problem posed above.

The fluid is assumed to be inviscid and incompressible and the flow irrotational. In two dimensions the velocity potential ϕ and the stream function ψ are required to satisfy

$$\nabla^2\phi=0, \qquad \nabla^2\psi=0. \tag{1}$$

The complex potential is defined as

$$\beta(z;\, t)=\phi(z;\, t)+\mathrm{i}\psi(z;\, t), \tag{2}$$

where $z=x+\mathrm{i}y$. Due to the analyticity of β in the fluid domain, Cauchy's theorem gives

$$\int_C \frac{\beta}{z-z_0}\,\mathrm{d}z=0, \tag{3}$$

where C is a closed contour (see Figure 2) consisting of the free surface, the open boundaries, the

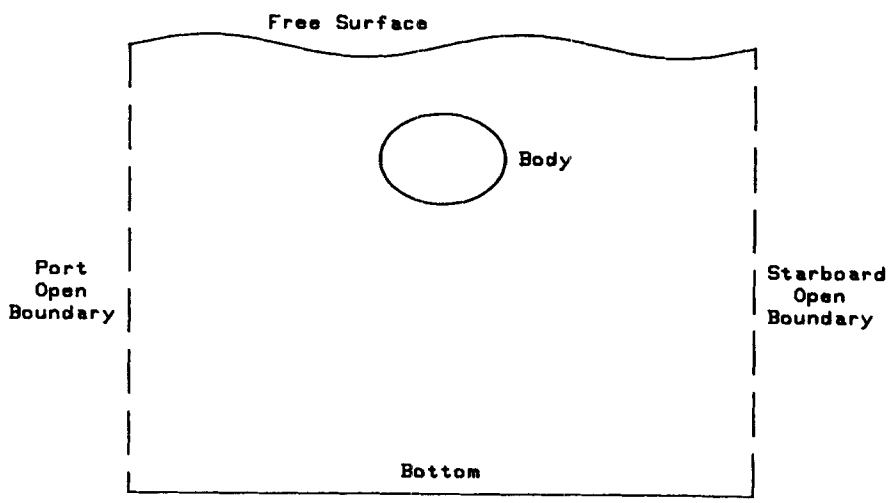

Figure 1. Definition sketch for the problem

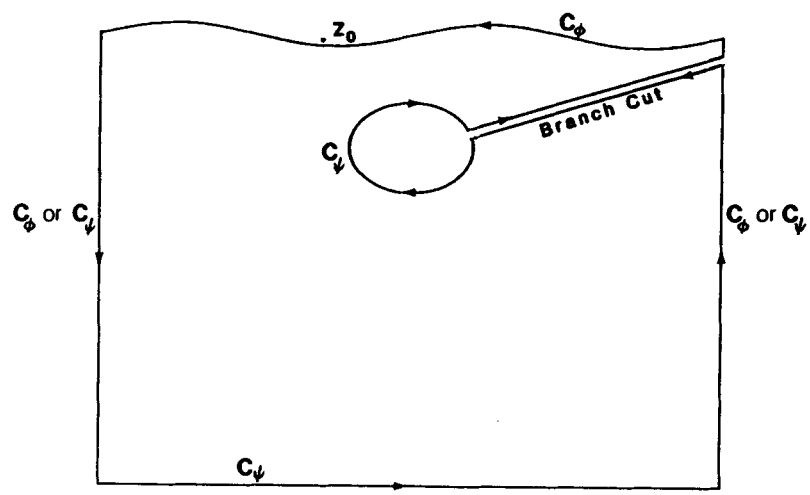

Figure 2. Closed contour for the problem

bottom and (with a branch cut if necessary) the body; z_0 is a point outside the contour. Letting the point z_0 approach C from the outside, equation (3) yields

$$i\alpha\beta(z_0)+\int_C \frac{\beta}{z-z_0}\,dz=0, \tag{4}$$

where α is the interior angle of the contour at the point z_0. If the contour is smooth at z_0, then $\alpha=-\pi$.

Let the contour $C=C_\phi+C_\psi$, where ϕ is known on C_ϕ and ψ is known on C_ψ. Then the real and imaginary parts of equation (4) yield Fredholm integral equations of the second kind as follows:

$$\alpha\psi(z_0;\,t)+\mathrm{Re}\left(\int_C \frac{\beta}{z-z_0}\,dz\right)=0 \tag{5a}$$

for z_0 on C_ϕ and

$$\alpha\phi(z_0;\,t)+\mathrm{Re}\left(i\int_C \frac{\beta}{z-z_0}\,dz\right)=0 \tag{5b}$$

for z_0 on C_ψ.

Boundary conditions

Free surface (C_ϕ boundary). Exact (non-linear) free surface conditions are satisfied by using Lagrangian marker particles on the free surface. The positions of the fluid particles at the free surface are integrated in time from the kinematic free surface condition

$$Dz/Dt=u+iv=w^*, \tag{6a}$$

where w^* is the complex conjugate of the complex velocity

$$w=u-iv=\partial\beta/\partial z.$$

The velocity potential on the free surface (which would become a boundary condition for the

boundary value problem at the next time step) at the position of the marker particles is found by integrating the Lagrangian form of the dynamic free surface condition[2]

$$D\phi/Dt = \tfrac{1}{2}ww^* - gy - p_s/\rho, \tag{6b}$$

where D/Dt is the material derivative, g is the gravitational constant, y is the free surface elevation, ρ is the fluid density and p_s is any externally applied pressure distribution on the free surface (usually taken as zero).

Bottom (C_ψ boundary). The bottom boundary condition is

$$\partial\phi/\partial n = 0. \tag{7a}$$

This may be satisfied by setting

$$\psi = \text{constant} \tag{7b}$$

and, in particular, this constant is chosen as zero.

Body (C_ψ boundary). The kinematic body boundary condition is

$$\partial\phi/\partial n = \partial\psi/\partial s = \mathbf{v}\cdot\mathbf{n} \tag{8a}$$

and

$$\mathbf{v} = \mathbf{v}_0 + \dot{\omega}\mathbf{k}\times\mathbf{R}, \tag{8b}$$

where $\mathbf{v}$ is the rigid body velocity at the body boundary and $\mathbf{n}$ is the body normal. Vinje and Brevig[4] show that the stream function can be integrated from equation (8a) to give

$$\psi(x, y; t) = u_0(y-y_0) - v_0(x-x_0) - \tfrac{1}{2}\dot{\omega}|\mathbf{R}|^2, \tag{8c}$$

where (u_0, v_0) are the components of sway and heave velocities, (x_0, y_0) represent the centre of roll of the body, $\dot{\omega}$ is the angular velocity and $\mathbf{R}$ is the position vector from the body boundary to the centre of the roll.

Thus if the forced motion of the body $u_0(t)$, $v_0(t)$, $\dot{\omega}(t)$ is known, the stream function value on the body boundary is available at all instants of time. The partial time derivative of the stream function at the body (which is needed for the determination of the pressures on the body) is available as

$$\begin{aligned}\partial\psi(x, y; t)/\partial t = {} & (y-y_0)\dot{u}_0 - (x-x_0)\dot{v}_0 - \tfrac{1}{2}|\mathbf{R}|^2\ddot{\omega} + u_0\phi_y - v_0\phi_x \\ & + [(u_0-\phi_x)(x-x_0) + (v_0-\phi_y)(y-y_0)]\dot{\omega}\end{aligned} \tag{8d}$$

Open boundaries. The most difficult part in the solution of two-dimensional non-linear flow problems is the treatment of the open boundaries where a radiation condition needs to be applied. In the time domain, for an initial value problem, a radiation condition is actually not necessary. A sufficient condition is to state that in the far field the disturbance is negligibly small. The implementation of such a condition is not practical (except for cases of non-propagative solutions at infinity using mapping techniques), for there would have to be a progressive domain expansion with time, leading to unreasonable computational costs. This consideration then implies the use of a truncated domain using 'open boundaries'. Thus the advantage of an initial value formulation is not available and suitable radiation conditions need to be furnished at these open boundaries. To solve the boundary value problem given by Fredholm integral equations (5a) and (5b), either the velocity potential ϕ or the stream function ψ should be known at the open boundary at each instant in time.

Determination of forces

The forces on the body are determined by integrating the pressure around the body. The dynamic pressure is given as

$$p/\rho = \partial\phi/\partial t - \tfrac{1}{2} ww^*. \tag{9}$$

Hence the values of $\partial\phi/\partial t$ have to be known on the body. This could be done either with backward differencing of the velocity potential with respect to time or a separate boundary value problem may be formulated for the analytic function $\partial\beta/\partial t$. This latter approach has been used, since the backward differencing scheme was found by this author and by Vinje and Brevig[4] to be numerically unstable.

The analyticity of the function $\partial\beta/\partial t$ yields from Cauchy's theorem

$$\int_C \frac{\partial\beta/\partial t}{z - z_0}\,\mathrm{d}z = 0 \tag{10a}$$

for z_0 outside the contour C. The contour C consists of C_{ϕ_t} where $\partial\phi/\partial t$ is known and C_{ψ_t} where $\partial\psi/\partial t$ is known and hence equation (10a) can be written as

$$\alpha \frac{\partial\psi}{\partial t}(z_0; t) + \mathrm{Re}\left(\int_C \frac{\partial\beta/\partial t}{z - z_0}\,\mathrm{d}z \right) = 0 \tag{10b}$$

for z_0 on C_{ϕ_t} and

$$\alpha \frac{\partial\phi}{\partial t}(z_0; t) + \mathrm{Re}\left(\mathrm{i} \int_C \frac{\partial\beta/\partial t}{z - z_0}\,\mathrm{d}z \right) = 0 \tag{10c}$$

for z_0 on C_{ψ_t}.

The free surface is part of C_{ϕ_t} from the Eulerian dynamic free surface condition derivable from equation (6b). The bottom is part of C_{ψ_t} since it satisfies the condition $\psi_t = 0$. The body boundary is part of C_{ψ_t} since ψ_t is known on the body from equation (8d). Once again for the boundary value problem for $\partial\beta/\partial t$ to be well posed, either ϕ_t or ψ_t should be known on the open boundaries.

A note on the method of solution

The boundary value problem for ϕ and ψ in terms of equations (5a) and (5b) yields Fredholm integral equations of the second kind. If the contour C is defined as $C = C_\phi + C_{\phi_n}$ where ϕ is known on C_ϕ and ϕ_n is known on C_{ϕ_n}, then Green's theorem gives

$$\phi(P) = \frac{1}{\pi} \int_C \left(\phi(Q) \frac{\partial}{\partial n} \log r(P, Q) - \frac{\partial\phi}{\partial n} \log r \right) \mathrm{d}s(Q). \tag{11}$$

Equation (11) is the solution for a boundary value problem given either ϕ or ϕ_n on C and is a Fredholm integral equation of the first kind. Vinje and Brevig[3, 4] state in the literature that the formulation based on ϕ and ψ is more stable because of the generally better characteristics of Fredholm integral equations of the second kind. It has been suggested that this accounts for the instability in the work of Longuet-Higgins and Cokelet.[2] However, it can be easily shown that equation (11) is derivable directly from equation (4) as follows:

$$\beta(z_0) = \frac{1}{\pi \mathrm{i}} \int_C \frac{\beta(z)}{z - z_0}\,\mathrm{d}z. \tag{12}$$

Let $z-z_0=re^{i\theta}$, $r=|z-z_0|$ and $\theta=\arg(z-z_0)$. Hence

$$\frac{dz}{z-z_0}=\frac{dr}{r}+id\theta;$$

i.e.

$$\phi(z_0)+i\psi=\frac{1}{\pi i}\int_C\left[(\phi(z)+i\psi)\left(\frac{dr}{r}+id\theta\right)\right]. \tag{13}$$

Taking the real part of equation (13),

$$\phi(x_0, y_0)=\frac{1}{\pi}\int_C\left(\phi d\theta+\psi\frac{dr}{r}\right). \tag{14}$$

Now

$$\int\phi d\theta=\int\phi\frac{\partial\theta}{\partial s}ds=-\int\phi\frac{\partial}{\partial n}\log r\,ds, \tag{15}$$

which follows from the Cauchy–Rieman equations for the analytic function $\log(z-z_0)$. Also

$$\int\psi\frac{dr}{r}=\int\psi d(\log r)=-\int\frac{\partial\psi}{\partial s}\log r\,ds+[\psi\log r]=\int\frac{\partial\phi}{\partial n}\log r\,ds, \tag{16}$$

since $[\psi\log r]$ equals zero over a closed contour. Substituting equations (15) and (16) into equation (14), we get

$$\phi(x_0, y_0)=\frac{1}{\pi}\int_C\left(\phi\frac{\partial}{\partial n}(\log r)-\frac{\partial\phi}{\partial n}\log r\right)ds \tag{17}$$

for a field point $P(x_0, y_0)$.

Thus equation (11) has been derived from equation (4) simply by using the Cauchy–Rieman equations. Hence equation (11), which is a Fredholm integral equation of the first kind, and equation (5), which is a Fredholm integral equation of the second kind, are both derived from equation (4). Equation (5) works with the velocity potential ϕ and the stream function ψ, while equation (11) works with the velocity potential ϕ and its normal $\partial\phi/\partial n$. The physical problem and the implementation of boundary conditions are identical. It is therefore difficult to see why equation (11) is any less stable than equation (5) as noted by Vinje and Brevig.[4] The instability observed in the work of Longuet-Higgins and Cokelet[2] is probably numerical.

Taking the imaginary part of equation (13) and using the C–R equations, one gets a formulation based on the stream function:

$$\psi(x_0, y_0)=\frac{1}{\pi}\int_C\left(\frac{\partial\psi}{\partial n}\log r-\frac{\partial}{\partial n}(\log r)\right)ds. \tag{18}$$

3. EXTENSION OF THE ORLANSKi CONDITION

It is often necessary to introduce artificial boundaries to limit the domain of computation. Boundary conditions are then needed at these artificial boundaries to ensure a unique solution. Moreover, the boundary conditions should be such that the solution so obtained will closely approximate the solution that would exist in the absence of the artificial boundary; i.e. the open boundary conditions should not distort the solution in the interior domain. The formulation of appropriate open boundary conditions has received much attention in the literature and a review of the various approaches is given by Jagannathan.[6]

For many physical problems the appropriate partial differential equation is hyperbolic in nature and the phenomena are characterized by wave propagation. Open boundary conditions for such problems are naturally based on the idea of wave absorption. For a time harmonic problem given by $\phi = \bar{\phi} e^{-ivt}$ (where $\bar{\phi}$ is complex), the appropriate boundary condition is the well known Sommerfeld condition[7]

$$\phi_x \mp ik\phi \to 0 \quad \text{as} \quad x \to \pm\infty \tag{19}$$

for two dimensions and k is the wave number corresponding to the frequency v. In the time domain, if the solution is expected in the form $\phi(x, y, t) = \phi(x - ct, y)$, where c is the phase velocity, then the Sommerfeld condition above may be written as

$$\phi_t + c\phi_x = 0. \tag{20}$$

This condition applied numerically is often known as the Orlanski condition.

In many problems the value of the phase velocity to be used is not known. Kreiss[8] dealt with the problem of unknown phase velocity by assuming $c = \Delta x/\Delta t$, where Δx and Δt are the spatial and temporal grid sizes. Pearson[9] obtained the phase velocity from the linearized dispersion relationship using only the dominant wave. Orlanski[10] suggested that the phase velocity, instead of being a constant value, should be numerically determined from neighbouring grid points.

The Orlanski condition in a non-dissipative neutrally stable form has been used by Chan.[11] Camerlengo and O'Brien[12] used the Orlanski scheme with minor modifications and concluded that while the modified scheme worked for some cases (free Kelvin waves), there was some reflection for other cases (forced Rosby waves). Han *et al.*[13] used a forward-time, upwind-space variation of the Orlanski condition for application to stratified flows. They concluded that the open boundary condition performed remarkably well, even for these parabolic problems. Ertekin[14] used the Sommerfeld condition directly to study the behaviour of long waves by using $c = \pm\sqrt{(gh_0)}$, where h_0 is the water depth.

An extension to the Orlanski scheme is now proposed. In initial value and unsteady flow problems the critical question is the value of the phase velocity to be used. With particular reference to the problem posed in Section 2, the outgoing behaviour of the velocity potential at the open boundaries is directly related to the free surface behaviour near those boundaries. We then postulate the following:

(a) The value of the phase velocity at the open boundaries is the value of the phase velocity on the free surface near those boundaries.
(b) The value of the phase velocity c at the free surface may be determined at any instant as

$$c = -\phi_t/\phi_x. \tag{21}$$

The Orlanski condition is implemented in the simulation as follows. Consider a point on the *free surface* close to the open boundary. At some time $t = t_0$ let the complex potential $\beta = \phi + i\psi$ and the value ϕ_t be known at this point. The value of $u = \phi_x$ is obtained by numerical differentiation with neighbouring free surface points. Hence, using equation (21), the value of the phase velocity c is obtained. Now at a point on the *open* boundary ϕ_x is obtained by spatial differentiation and hence, using equation (20), the value of ϕ_t and by integration the value ϕ are obtained. With this known value of ϕ on the open boundary and using the free surface, bottom and body boundary conditions, the boundary value problem is solved to obtain ψ on the open boundary. For the next instant in time the free surface condition gives a new value of ϕ_t and β on the free surface and the process continues.

However, there could be problems in estimating c when ϕ_t, $\phi_x \to 0$. To avoid this problem and to get a robust estimate of c, a 'numerical scanner' was implemented in the procedure. This

scanner merely computes c according to equation (21) at several points close to the open boundary but ignoring points where $\phi_t, \phi_x \to 0$. The average phase velocity c is then obtained and used for the open boundary condition in equation (20).

This approach to the implementation of an Orlanski boundary condition was tested using a small-amplitude progressive free surface wave of period 2π in a water depth of 101·16 ft. At time $t=0$ the wave configuration and its velocity potential were taken as initial conditions. The simulation was carried out with the Orlanski open boundary condition implemented at the port and starboard boundaries and it was found that this progressive wave could be simulated without distortion. Figure 3 shows the values of the phase velocity obtained using equation (21) at free surface nodes 1, 8, 15, 23, 30, 37, 45 and 50 at three instants in time. It is to be noted that the numerically determined phase velocities over the length of the wave are quite close to the theoretical value of 32·2 ft s^{-1}.

The stability characteristics of the present approach for determination of the phase velocity will differ from that of Orlanski[10] who specified an upper bound as follows:

$$c = \Delta x/\Delta t \quad \text{if} \quad -\phi_t/\phi_x > \Delta x/\Delta t, \tag{22}$$

where Δx is the spatial grid size and Δt is the time step. Orlanski[10] enforced this bound since both ϕ_t and ϕ_x were determined through numerical differentiation. In the present approach ϕ_x is determined through numerical differentiation but ϕ_t is obtained from the dynamic free surface condition. Noting that

$$D\phi/Dt = \phi_t + ww^* \tag{23}$$

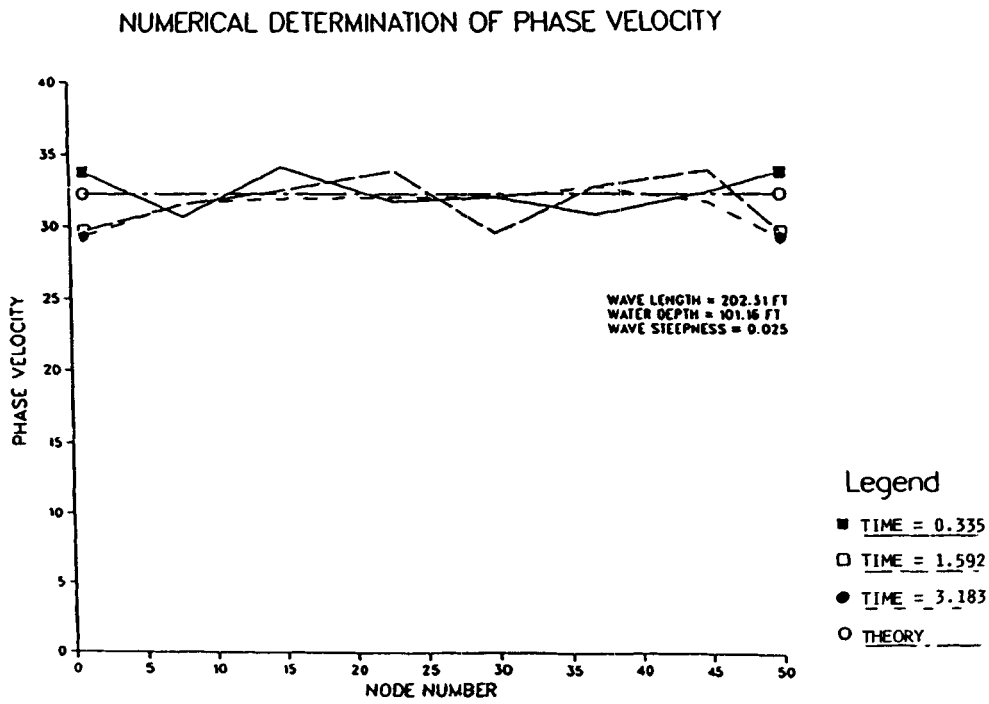

Figure 3. Phase velocity determination using the extended Orlanski condition for a small-amplitude progressive wave

and using equations (6b) and (21), we get

$$c = \frac{\frac{1}{2}ww^* + gy + P_s/\rho}{\phi_x} \tag{24}$$

$$= \frac{\frac{1}{2}(\phi_x^2 + \phi_y^2) + gy + P_s/\rho}{\phi_x}. \tag{25}$$

Thus the temporal grid size does not appear explicitly in the determination of the phase velocity at a given instant in time. This implementation of the Orlanski condition has been used for the case of a submerged body executing forced oscillation close to the free surface and the results are given in the next section.

4. RESULTS AND DISCUSSION

Freely moving steep waves

The behaviour of a freely moving steep wave investigated by McIver and Peregrine[15] is analysed to determine the characteristics of the simulation process. The wave is considered spatially periodic at every wavelength and is imposed with an initial steepness that forces it to plunge within one period. Figure 4 shows the evolution of the wave using a four-stage non-iterative Adam's predictor–corrector method[16] for integration over time. Figure 5 shows energy and momentum checks. It is seen from Figure 5 that there is a slow but steady loss of energy and momentum from the system. This arises from the presence of artificial viscosity[17] induced into the system by the use of numerical (and hence approximate) space and time derivatives. The same wave was simulated using a fourth-order Runge–Kutta procedure[16] for the entire process. The variation of energy and momentum for the Runge–Kutta method is given in Figure 6, while Figure 7 shows a comparison of wave profiles for the two methods at one instant in time. It is noted that dissipation of energy is less for this procedure compared with the Adam's method. It is hypothesized by the author that this is related to the Adam's method using spatial derivatives of three lagging time steps and thus accumulating errors whereas the Runge–Kutta method is self-starting at each time step.

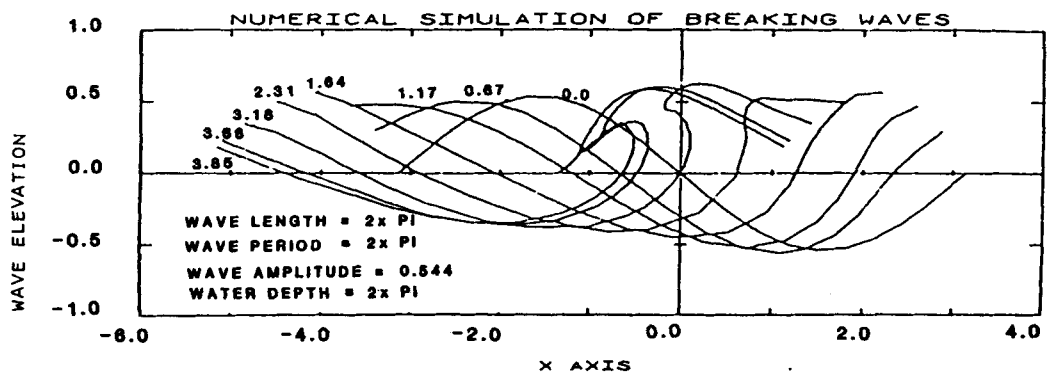

Figure 4. Behaviour of the freely moving steep wave analysed by McIver and Peregrine[15]

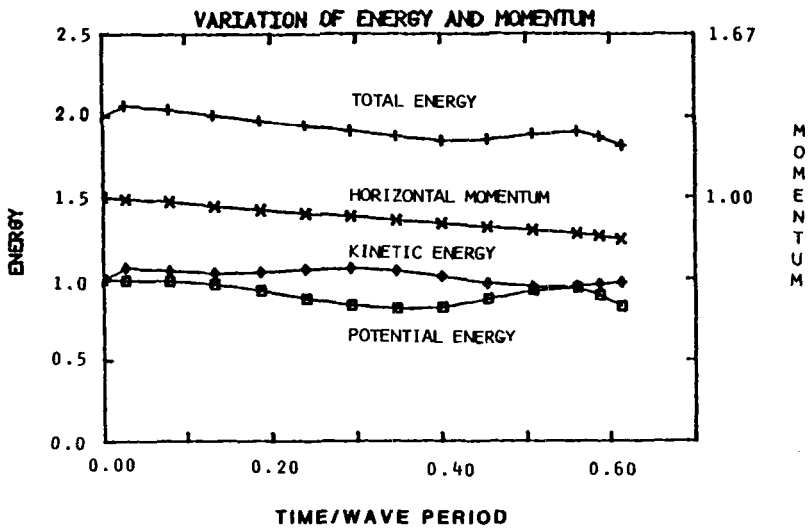

Figure 5. Energy and momentum checks with simulation using Adam's predictor–corrector method

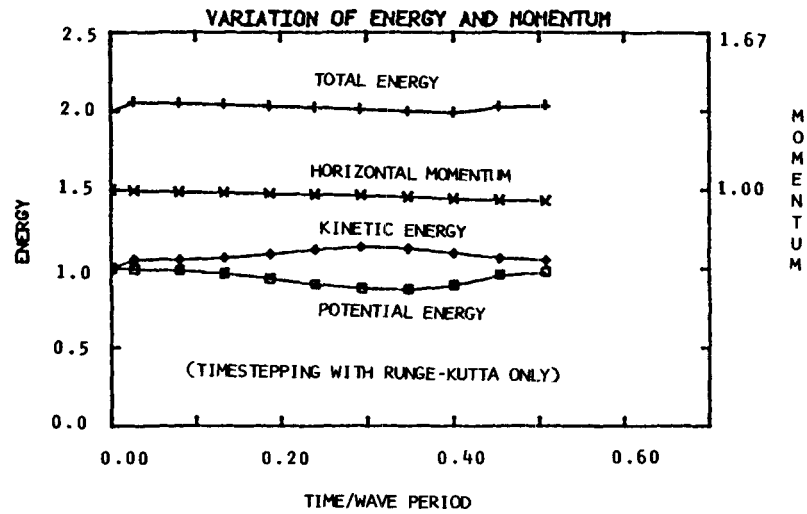

Figure 6. Energy and momentum checks with simulation using Runge–Kutta method

Waves over a submerged body

This subsection deals with two aspects. The first part is a comparison of the results of simulation with linear theory and experimental data for waves of very small steepness passing a submerged cylinder. This serves to assess the nature and effectiveness of the simulation procedure. The second part deals with the case of extreme waves over a submerged cylinder and a comparison with linear theory predictions is provided. In both cases the axis of the cylinder is parallel to the wave crests and spatial periodicity is imposed as the open boundary condition.

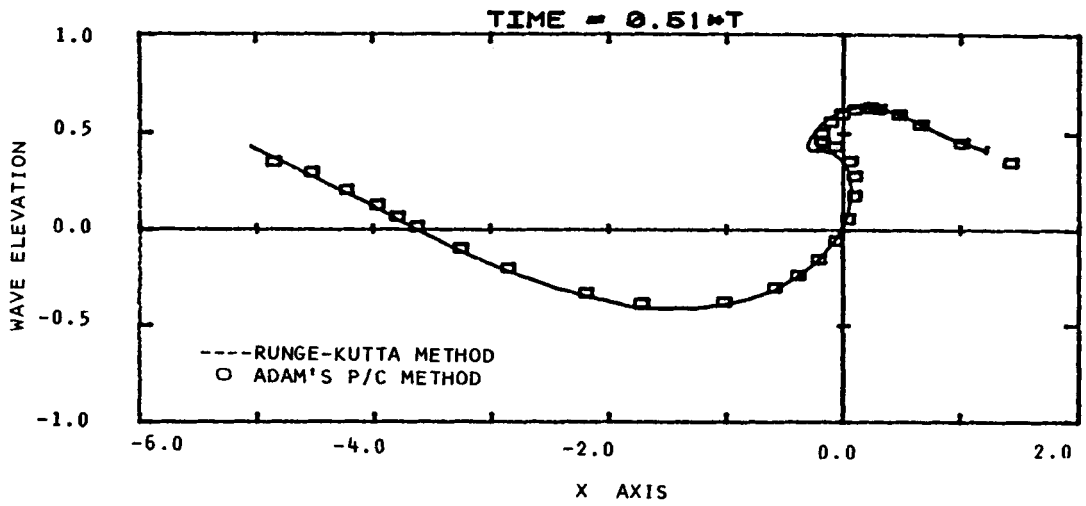

Figure 7. Comparison of wave profiles at $t=0{\cdot}51T$ for simulation using Adam's and Runge–Kutta methods

Two numerical experiments were conducted for the case of small-steepness waves incident upon a submerged 0·36 m (14 inch) long cylinder of radius 0·10 m (0·33′) in water of depth 1·60 m (5·25′). The comparison is with the theoretical results of Ogilvie[18] and the experimental work of Chiu[19]. The results of Ogilvie are for first-order forces and the second-order steady force (which depends only on the first-order potential) and are available as a convergent infinite series. The force function (following Chiu) is defined as

$$\text{Force function} = \text{Force}/(2\pi\rho g A_i/k), \tag{26}$$

where A_i is the incident wave amplitude and k is the wave number.

Note: In the results that follow in Figures 10, 12 and 13 some room for confusion exists, since time-variant and non-time-variant quantities are shown. For the experimental results only the first-order amplitude and the 'steady' (not time-variant) second-order drift force are available and these have been shown as constants. The theoretical results of Ogilvie are shown as total time-variant force (linear first-order time-variant force superposed on a steady second-order drift force). The theoretical steady second-order drift force is also shown (as a constant value). The basis for comparison is therefore the shape of the time-variant force curves from simulation and theory and the total amplitude over one cycle for simulation, theory and experiment.

The first case deals with the centre of the cylinder submerged at 0·13 m (0·425′) subjected to a wave of period 1·432 s and amplitude 0·01 m (0·038′). Figure 8 shows the horizontal and vertical simulation forces. The phase angle between horizontal and vertical forces is more than the theoretical value of 90°. The vertical force appears to be less completely periodic than the horizontal force. Figures 9 and 10 show the comparisons of horizontal and vertical forces for simulation, theory and experiment. In both cases simulation compares better with theory than with experiment. The simulation is out of phase w.r.t. theory (due to the formulation as an initial value problem where at $t=0^-$ there was no cylinder and no diffraction) but catches up with theory as time progresses. For apparently the same reason, simulation under-predicts the vertical force initially but is fairly accurate at the end of one period.

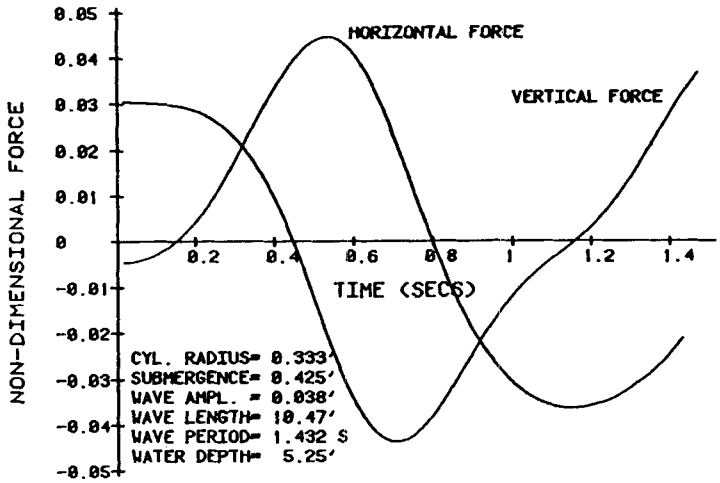

Figure 8. Vertical and horizontal forces from simulation for cylinder of radius 0·33′ at submergence 0·425′

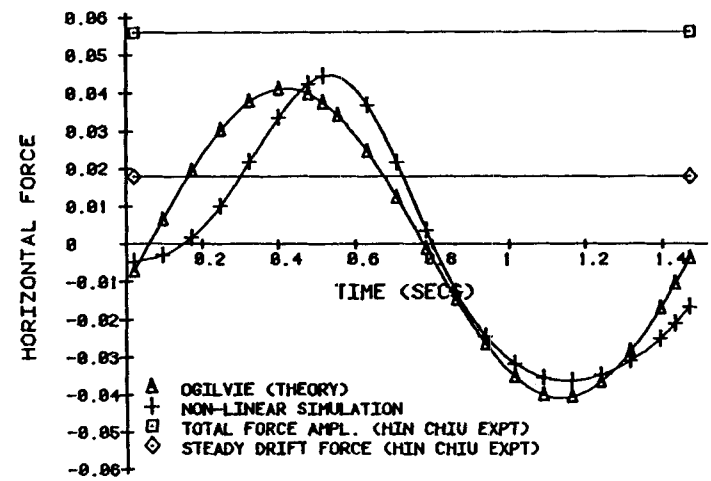

Figure 9. Comparison of horizontal forces from simulation, theory and experiment

The next case deals with the cylinder submerged to 0·20 m (0·667′) subjected to a wave of period 0·904 s and amplitude 0·01 m (0·040′). Figure 11 shows the vertical and horizontal simulation forces for this problem. Here the phase between vertical and horizontal forces is almost exactly 90° as predicted by linear theory. The vertical force amplitude is slightly higher than the horizontal force amplitude, as is also seen in Chiu's experiment, although linear theory predicts equal amplitudes. The sinusoidal response of the simulation forces is quite remarkable considering that it has been solved as an initial value problem. It is to be noted that the amplitudes of the second cycle are smaller than the first. This is because the computational domain was limited to one wavelength (to reduce computational costs) and space periodicity was used as the open

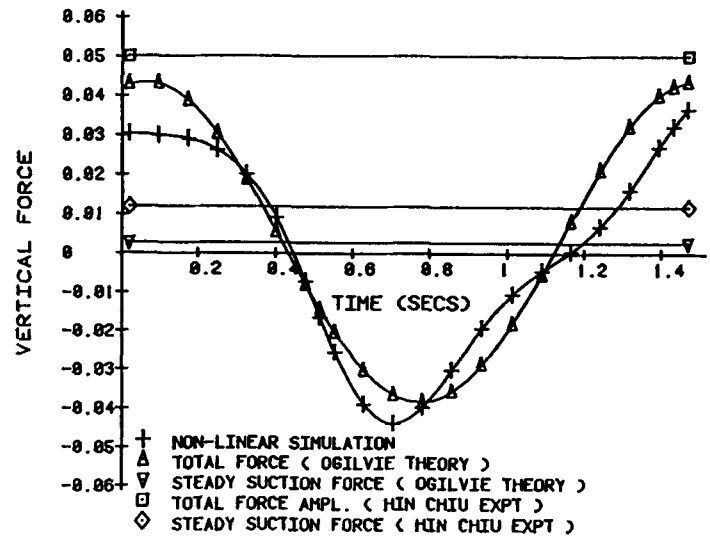

Figure 10. Comparison of vertical forces from simulation, theory and experiment

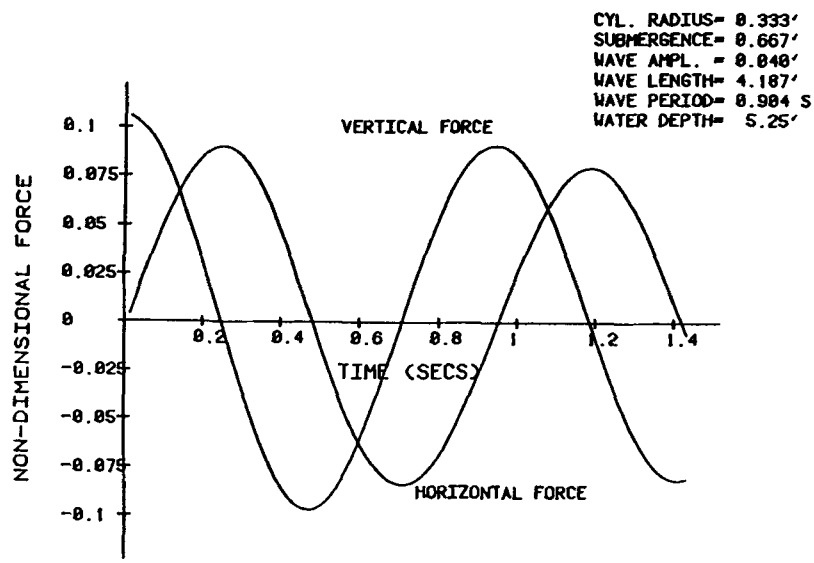

Figure 11. Vertical and horizontal forces from simulation for cylinder of radius 0·33′ at submergence 0·67′

boundary condition. Space periodic open boundary conditions lead to mathematically well posed boundary value problems and have been used by Longuet-Higgins and Cokelet[2] and Vinje and Brevig.[3] They do not constitute physically correct open boundary conditions as they imply that the problem is continued in a periodic sense to infinity in both directions. However, these boundary conditions are easy to use and give acceptable results when the open boundaries are situated far enough from the disturbance in the computational domain. Figures 12 and 13 show

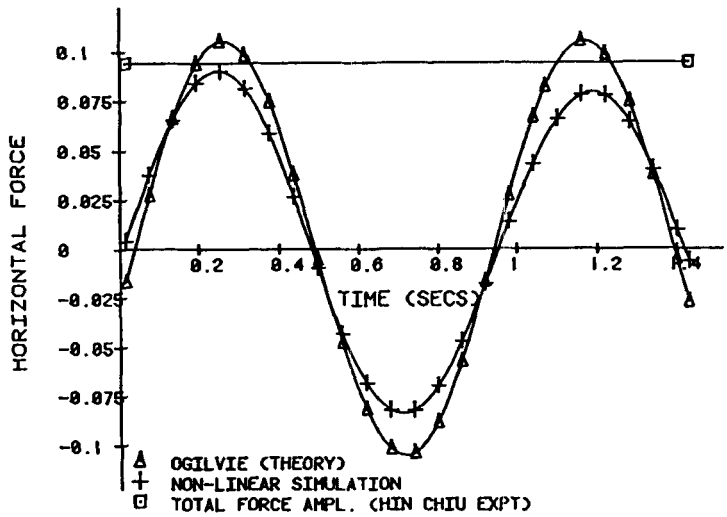

Figure 12. Comparison of horizontal forces from simulation, theory and experiment

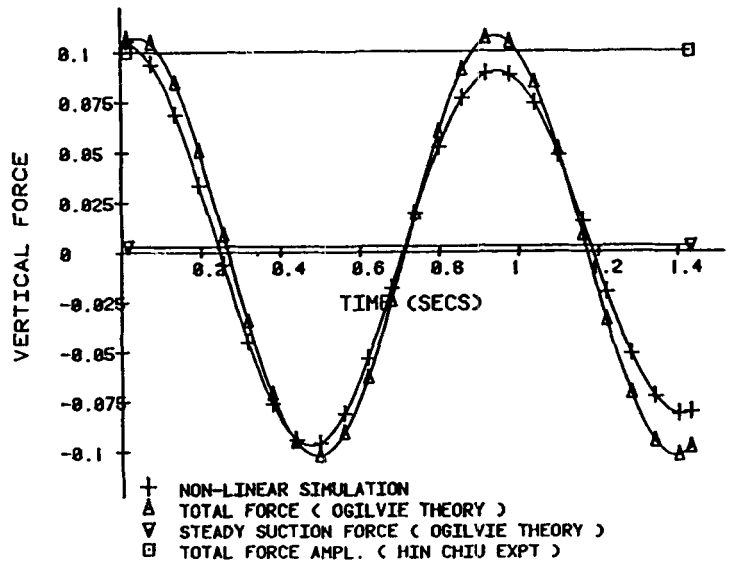

Figure 13. Comparison of vertical forces from simulation, theory and experiment

comparisons of horizontal and vertical forces for simulation, experiment and theory. All three compare very well with each other, with the experimental value falling in between the simulation and theoretical values. There is almost no phase difference between the simulation and theoretical force components. In general force computations from simulation compare very well with results from experiment and theory. The agreement between simulation, theory and experiment is particularly good at deeper submergence. This leads to the consideration that certain anomalous

behaviour (for instance the vertical force for the first case) predicted by simulation for shallow submergence may actually exist but is not predicted by linear theory.

We next consider the case of a steep wave passing a submerged stationary circular cylinder. The cylinder has a diameter of 10 m and the water depth is 60 m. The wave is of length 110 m and the amplitude is 10 m, giving a steepness of 0·182. If this wave were time-stepped without the body in flow, it would become a plunging breaker in about five seconds. Figure 14 shows the wave passing over the cylinder placed 20 m below the undisturbed free surface. It is noticed that the cylinder serves to accelerate the breaking process and the wave now spills over in around three seconds. A comparison of hydrodynamic pressure profiles around the cylinder for the cases of non-linear simulation and linear theory without diffraction showed that the pressures at the bottom half of the cylinder are still well predicted by linear theory, while for the upper half linear theory underestimates quite significantly. To clarify the effect of cylinder proximity to the free surface, the same wave was re-run with the cylinder placed 40 m below the free surface. A comparison of pressure profiles for this case showed that the peak dynamic pressure ratio of the simulation value to the linear theory value is smaller for this case, indicating that pressure attenuation is faster for non-linear simulation than for linear theory.

We next turn our attention to a comparison of non-linear forces with the inertial force component of Morison's equation. The context of such a comparison is that, given the diameter to wavelength ratio for this problem, the typical offshore industry practice would be to use Morison's equation to determine the force rather than linear diffraction theory. The drag force, being of viscous origin, is not considered and the focus is on the inertial force term. Figure 15 is a plot of the non-linear horizontal force compared with the linear Morison inertial force with various inertia coefficient (C_m) values. It is seen that the peak force is best approximated for a C_m value of 2·5. Noting that the theoretical asymptote for C_m is 2·0, this implies that the linear wave theory severely underestimates the local acceleration. Figure 16 shows a similar comparison for the vertical hydrodynamic force. In this case the C_m value required using linear wave theory to predict the peak force is about 3·2. Thus it appears that the vertical force is affected more than the horizontal force by the effects on free surface non-linearity and cylinder proximity to the free surface.

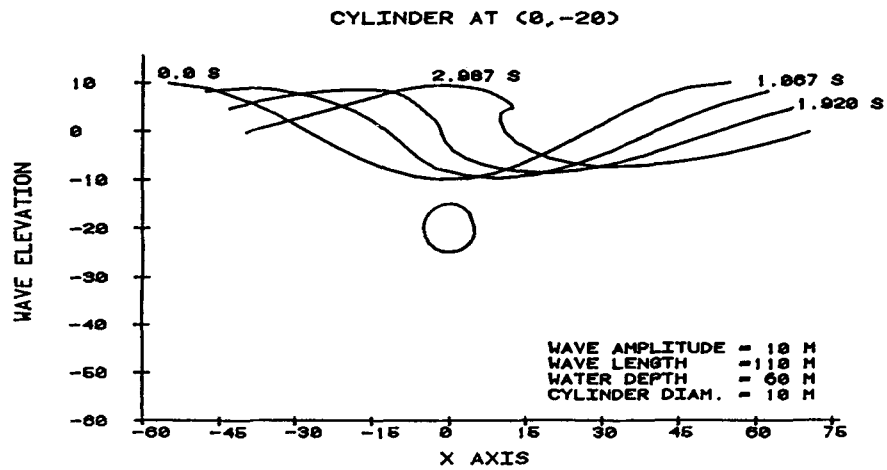

Figure 14. Steep wave of amplitude 10 m and wavelength 110 m passing a cylinder of radius 10 m at submergence 20 m

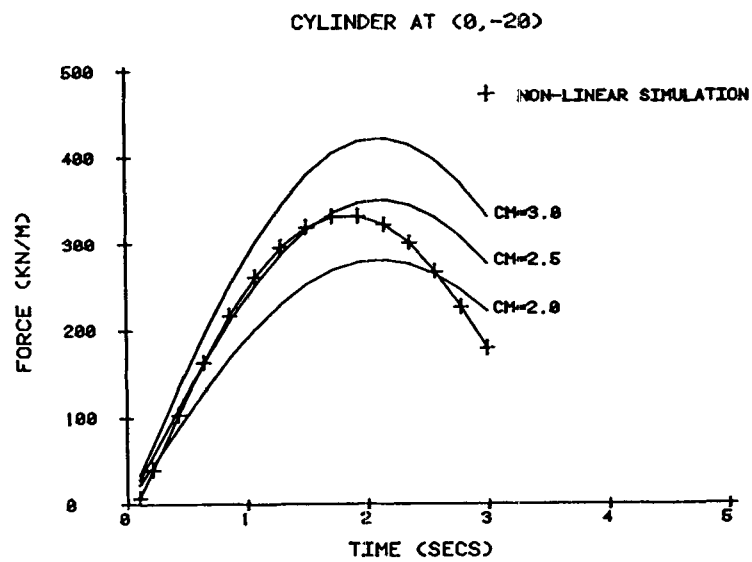

Figure 15. Comparison of horizontal forces from simulation and Morison's equation (inertial term)

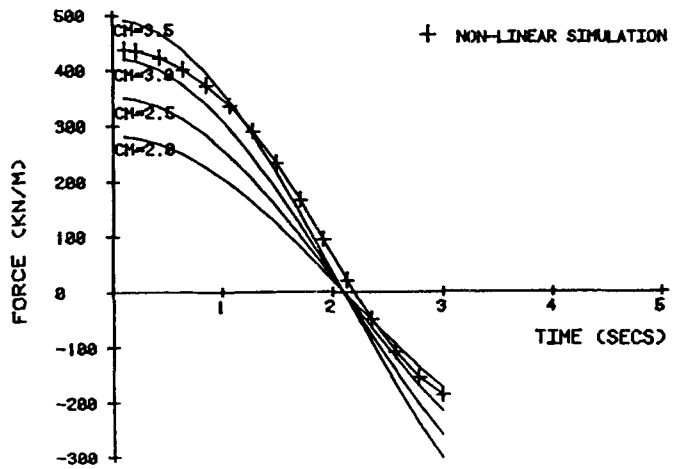

Figure 16. Comparison of vertical forces from simulation and Morison's equation (inertial term)

Forced body motion

This subsection deals with the radiation problem caused by the forced motion of a body. Of particular interest is the behaviour of the open boundary condition based on the extension of the Orlanski condition. The body was taken as a circular cylinder of radius 0·30 m (1·0′) submerged with its axis horizontal to a depth of (0·4 m) (1·3′) at its centre. The bottom was taken as uniformly flat at a depth of 1·60 m (5·25′) and the body was oscillated sinusoidally in heave at a frequency of 6·261 rad s^{-1}. Both the open boundaries were considered and were located at a distance of 2·39 m (7·5′) from the body.

Figures 17 and 18 show the values of the numerically determined phase velocities near the port and starboard open boundaries. Initially the phase velocities are high, corresponding to long waves generated as the body moves from rest. The numerical phase velocities converge to the linear steady-state value after about two periods of oscillation. Figure 19 shows four free surface profiles about one period apart. Figure 20 provides a comparison of the vertical force on the body obtained by simulation and the linear theory of Ogilvie.[18] The two compare very well and the simulation value reaches steady state after about two oscillations.

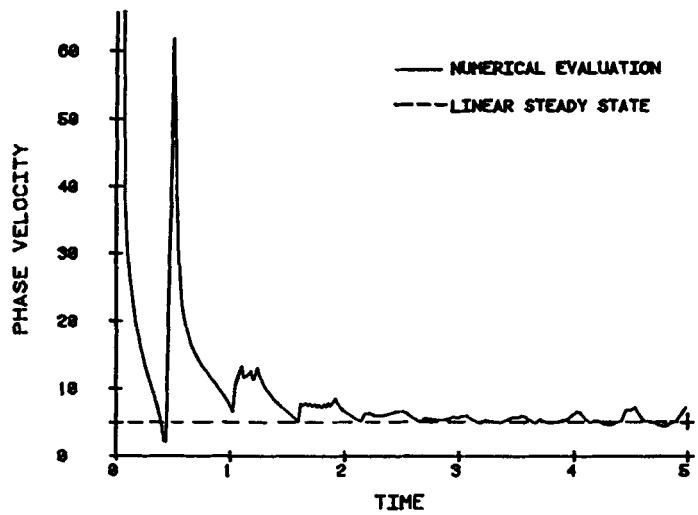

Figure 17. Phase velocity using the extended Orlanski boundary condition at the port (left-hand side) boundary for forced body motion problem

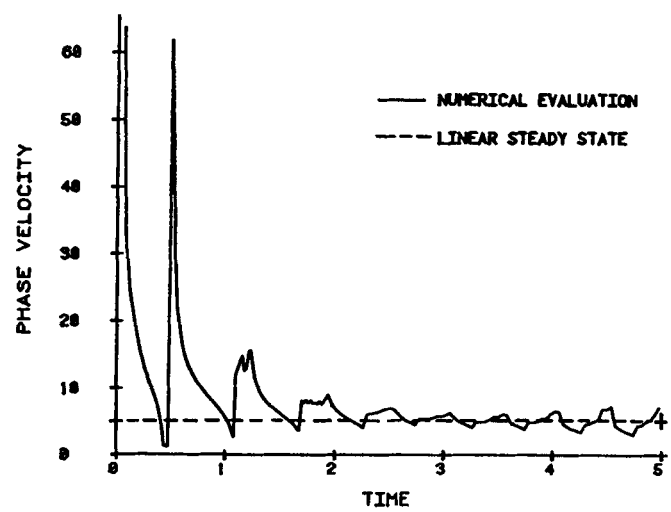

Figure 18. Phase velocity using the extended Orlanski condition at the starboard (right-hand side) boundary

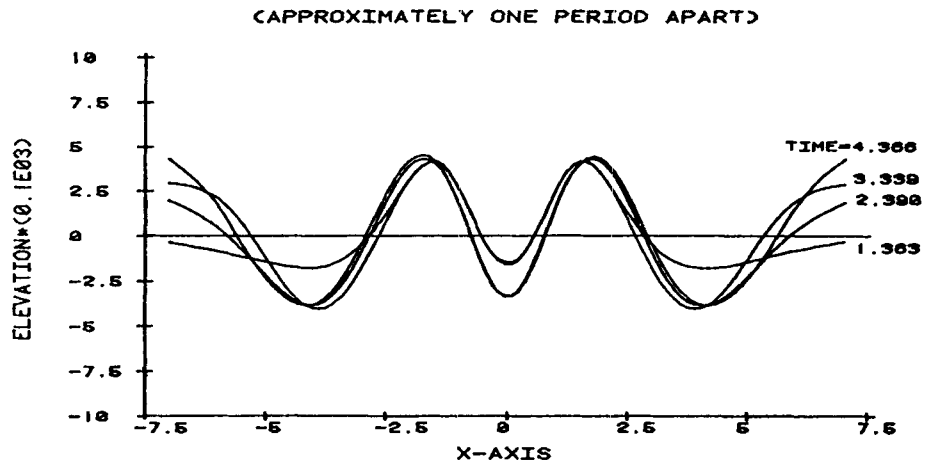

Figure 19. Free surface elevations for the forced body motion problem

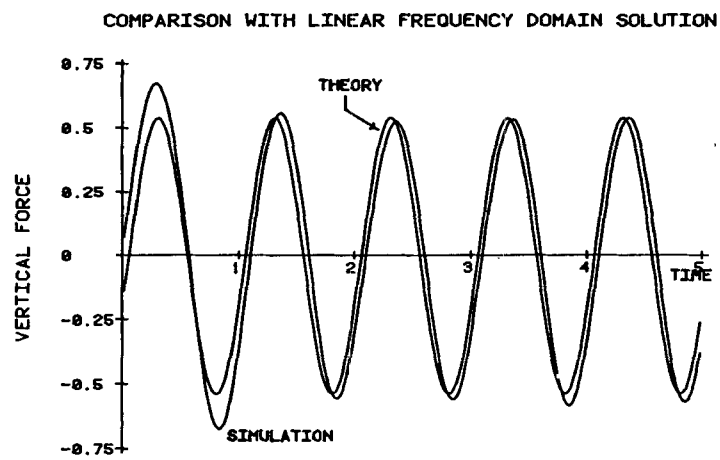

Figure 20. Comparison of vertical forces from simulation and frequency domain theory

5. CONCLUSIONS

Three categories of spatially two-dimensional free surface problems have been analysed in this paper—namely, freely moving steep waves, waves over a submerged body and forced body motion. The main complexities of these problems are the proper treatment of the non-linear free surface conditions, the body boundary condition for large motions and the radiation or open boundary condition. It has been shown here that the simulation method imbedded in a boundary integral formulation is very suitable for the analysis of these problems. Yeung[1] shows that for two-dimensional problems the boundary integral formulation is computationally less intensive than the finite element or finite difference methods. Other problems which could be successfully analysed using this method are waves breaking against a breakwater, large motions of tanks

containing a fluid, roll motions of a ship, non-linear forces on offshore structures, etc. The extension of this method to three-dimensional problems is straightforward, although computationally intensive.

Of particular current interest is the treatment of the open boundary condition. For linear problems this is the radiation condition which is well known. For non-linear problems no general open boundary conditions are known so far. Many individual approaches have emerged, such as those of Hedstrom[20] for non-linear hyperbolic systems, Rudy and Strikwerda[21] for Navier–Stokes flows and Enquist and Majda[22] for a general class of wave equations. In this paper an extension of the Orlanski scheme has been proposed and verified for the case of a freely moving gravity wave and an oscillating body. This condition appears quite non-reflective and is probably satisfactory for many practical applications. A more theoretical approach to the non-linear open boundary condition problem has been proposed by Jagannathan.[6] It should be noted that for many three-dimensional problems the open boundary condition may be linearized based on the consideration of energy dissipation. In contrast, with two-dimensional non-linear problems there is no energy dissipation with distance and hence in principle the open boundary condition at any distance from the disturbance remains non-linear.

ACKNOWLEDGEMENTS

This work forms a part of the author's Ph.D. Dissertation[6] and was done under the guidance of Prof. W. C. Webster, which is gratefully acknowledged. The author would like to thank Prof. Ronald Yeung and Dr. T. Vinje for their advice and assistance. The financial support given by the Department of Naval Architecture and Offshore Engineering, U. C. Berkeley is acknowledged with gratitude.

APPENDIX: NOTATION

A_i	incident wave amplitude
C	contour for the boundary value problem
c	phase velocity
g	acceleration due to gravity
i	$\sqrt{-1}$
$\mathbf{k}$	unit vector normal to x–y plane
k	wave number
P, Q	generic points on the contour C
p	pressure
p_s	pressure at the free surface
r	polar radius
$\mathbf{R}$	position vector
u	velocity component in the x-direction
u_0	sway velocity of the body
v	velocity component in the y-direction
v_0	heave velocity of the body
w	complex velocity $u-iv$
x, y	Cartesian co-ordinates
x_0, y_0	location of the centre of roll of the body
z	point in the complex plane defined as $z=x+iy$
α	included angle
β	complex potential defined as $\beta=\phi+i\psi$

θ	angle in polar co-ordinates
ω, $\dot{\omega}$, $\ddot{\omega}$	roll angle, roll velocity, roll acceleration
ν	harmonic frequency
ρ	density of fluid
ϕ	velocity potential
ϕ_n	velocity along direction n
ψ	stream function
C_ϕ	part of contour C where velocity potential θ is known
C_ψ	part of contour C where stream function ψ is known
C_{ϕ_n}	part of contour C where ϕ_n is known
*	denotes complex conjugate

REFERENCES

1. R. W. Yeung, 'Numerical methods in free-surface flows', *Amer. Rev. Fluid Mech.*, **14,** 395–442 (1982).
2. M. S. Longuet-Higgins and E. D. Cokelet, 'The deformation of steep surface waves on water, I. A numerical method of computation', *Proc. Roy. Soc. Lond. A*, **350,** 1–26 (1976).
3. T. Vinje and P. Brevig, 'Breaking waves on finite water depths, A numerical study', *Ships in Rough Seas (SIS) Report*, Division of Marine Hydrodynamics, Norwegian Institute of Technology, 1980.
4. T. Vinje and P. Brevig, 'Nonlinear two-dimensional ship motion', *SIS Report*, Norwegian Institute of Technology, 1980.
5. T. Vinje and P. Brevig, 'Nonlinear ship motions', *Proc. 3rd Int. Conf. on Numerical Ship Hydrodynamics*, Paris, 1981.
6. S. Jagannathan, 'Nonlinear free surface flows and open boundary conditions', *Ph.D. Dissertation*, University of California, 1985.
7. F. John, 'On the motion of floating bodies, II', *Commun. Pure Appl. Math.*, **3,** (1950).
8. H. O. Kreiss, *Proc. Symp. at University of Wisconsin*, Wiley, New York, 1966.
9. R. A. Pearson, *J. Atmos. Sci.* **31,** (1974).
10. I. Orlanski, 'A simple boundary condition for unbounded hyperbolic flows', *J. Comput. Phys.* **21,** 251–269 (1976).
11. R. K. C. Chan, 'Finite difference simulation of the planar motion of a ship', *Proc. 2nd Int. Conf. on Numerical Ship Hydrodynamics*, Berkeley, 1977.
12. A. L. Camerlengo and J. J. O'Brien, 'Open boundary conditions in rotating fluids', *J. Comput. Phys.*, **35,** 12–35 (1980).
13. T. Y. Han, J. C. S. Meng and G. E. Innis, 'An open boundary condition for incompressible stratified flows', *J. of Comput. Phys.* **49,** 276–297 (1983).
14. R. C. Ertekin, 'Soliton generation by moving disturbances in shallow waters: theory, computation and experiment', *Ph.D. Dissertation*, University of California at Berkeley, 1984.
15. P. McIver and D. H. Peregrine, 'Comparison of numerical and analytical results for waves that are starting to break', *Proc. Symp. on Hydrodynamics in Ocean Engineering*, Norwegian Institute of Technology, 1981.
16. R. W. Hornbeck, *Numerical Methods*, Quantum Publishers Inc., New York, 1975.
17. P. J. Roache, *Computational Fluid Dynamics*, Hermosa Publishers, Albuquerque, 1980.
18. T. F. Ogilvie, 'First and second order forces on a cylinder submerged under a free surface', *J. Fluid Mech.*, **16,** 451–472 (1963).
19. H. Chiu, 'Diffraction of water waves by a circular cylinder', *Report No. NA-73-4*, College of Engineering, University of California, Berkeley, 1973.
20. G. W. Hedstrom, 'Nonreflecting boundary conditions for nonlinear hyperbolic systems', *J. Comput. Phys.*, **30,** 222–237 (1979).
21. D. H. Rudy and J. C. Strikwerda, 'A nonreflecting outflow boundary for subsonic Navier–Stokes calculations', *J. Comput. Phys.*, **36,** 55–70 (1980).
22. B. Engquist and A. Majda, 'Absorbing boundary conditions for the numerical simulation of waves', *Math. Comput.*, **31,** No. 139, 629–651 (1977).